

A STUDY OF FLUX VECTOR SPLITTING SCHEME APPLIED TO INVISCID COLD GAS HYPERSONIC FLOW SIMULATIONS

Farney Coutinho Moreira, farney.coutinho@gmail.com
Instituto Tecnológico de Aeronáutica - ITA
João Luiz F. Azevedo, joaoluiz.azevedo@gmail.com
Instituto de Aeronáutica e Espaço - CTA/IAE/ASA-L

Abstract.
A comparison of five different spatial discretizations schemes is performed considering a typical high speed flow application. A fully explicit, 2nd order accurate, 5-stage, Runge-Kutta time stepping scheme is used to perform the time march of the flow equations. The algorithms studied include 1st- and 2nd-order van Leer and Liou flux-vector splitting schemes. A technique that allows an excellent convergence acceleration of a numerical method is the multigrid procedure.The schemes here discussed are applied to the solution of hypersonic inlet flows. The inlet entrance conditions are varied from a freestream Mach number $M_\infty = 4$ up to $M_\infty = 12$, in order to test the schemes implemented for a wide range of possible inlet operating conditions. The results included in the present paper only considered inviscid computations,and the fluid was treated as a perfect gas, hence, no chemistry is taken into account.
Keywords: *CFD, Upwind, Unstructured*

1. INTRODUCTION

Upwind schemes take into account physical properties of the flow in the discretization process and they have the advantage of being naturally dissipative. Flux vector splitting methods introduce the information of the sign of the eigenvalues in the discretization process, and the flux terms are split and discretized according to the sign of the associated propagation speeds. Steger and Warming(1981) make use of the homogeneous property of the Euler equations and split the flux vectors into forward and backward contributions by splitting the eigenvalues of the Jacobian matrix into non-negative and non-positive groups. The split flux contributions are, then, spatially differenced according to one-sided upwind discretizations. However, these forward and backward fluxes are not differentiable when an eigenvalue changes sign, and this can produce oscillations at sonic points. In order to avoid these oscillations, van Leer(1982) defines a continuously spatially differenced flux vector splitting scheme that leads to smoother solutions at sonic points.

In the present work, the interface fluxes are calculated by five different algorithms, including a central difference-type scheme, van Leer (van Leer, 1982) and Liou (Liou, 1996) flux vector splitting schemes. In the central difference case, the interface fluxes are obtained from an average vector of conserved variables at the interface, which is calculated by straightforward arithmetic averages of the vector of conserved variables on both sides of the interface. For the first-order van Leer scheme, the interface fluxes are obtained by van Leer's formulas and they are constructed using the conserved properties for the i-th control volume and its neighbor across the given interface. The second order scheme considers a MUSCL approach Anderson et al. (1986), that is, the interface fluxes are formed using left and right states at the interface, which are linearly reconstructed by primitive variable extrapolation on each side of the interface. The extrapolation process is effected by a limiter in order to avoid the creation of new local extrema. The first- and second-order Liou schemes consider that the convective operator can be written as a sum of the convective and pressure terms(Liou, 1996). The second-order scheme also considers a MUSCL approach. Time march uses a fully explicit, 2nd-order accurate, five-stage Runge-Kutta time stepping scheme. Computations using a fine unstructured mesh are compared with other two large meshes in order to assess the quality of the solutions calculated by the different schemes implemented and in order to analyze the mesh influence in the capture of the flow features of interest.

A 3-D inlet configuration which is representative of some proposed inlet geometries for a typical transatmospheric vehicle is considered. The inlet entrance conditions are varied from a freestream Mach number $M_\infty = 4$ up to $M_\infty = 12$ in order to test the schemes implemented for a wide range of possible inlet operating conditions. The fluid was treated as a perfect gas and, hence, no chemistry was taken into account. From a physical standpoint, the present simulations are typical of cold gas flows which are usually achieved in experimental facilities such as gun tunnels. This is certainly not representative of actual flight conditions in which dissociation and vibrational relaxation are important phenomena, especially for the higher Mach number cases. However, it is a necessary step in order to construct a robust code to deal with the complete environment encountered in actual flight.

2. Theoretical Formulation

The flows of interest in the present context are modeled by the compressible Reynolds-averaged Navier-Stokes (RANS) equations. These equations can be written, considering the perfect gas assumption, as

$$\frac{\partial Q}{\partial t}+\frac{\partial E_e}{\partial x}+\frac{\partial F_e}{\partial y}+\frac{\partial G_e}{\partial z}=\frac{\partial E_v}{\partial x}+\frac{\partial F_v}{\partial y}+\frac{\partial G_v}{\partial z}\,, \qquad Q=\left[\begin{array}{ccccc}\rho & \rho\,u & \rho\,v & \rho\,w & e\end{array}\right]^{\mathrm{T}}\,. \tag{1}$$

where Q is the dimensionless vector of conserved variables, ρ is the fluid density, u, v and w are the Cartesian velocity components, e is the fluid total energy per unit volume, p is the pressure, R_e is the Reynolds number, M_∞ is the free stream Mach number and $\tau_{kx}, \tau_{ky}, \tau_{kz}$ is the stress tensor. In this work, all the variables arenon-dimensionalized according to (Pulliam, 1980). The E_e, F_e and G_e terms are the dimensionless inviscid flux vectors and E_v, F_v and G_v are the dimensionless viscous flux vectors, which can be written as

$$A_e=\left\{\begin{array}{c}\rho\,C\\ \rho\,uC+\delta_{kx}p\\ \rho\,vC+\delta_{ky}p\\ \rho\,wC+\delta_{kz}p\\ (e+p)\,C\end{array}\right\}, \qquad A_v=\frac{M_\infty}{Re}\left\{\begin{array}{c}0\\ \tau_{kx}\\ \tau_{ky}\\ \tau_{kz}\\ \beta_k\end{array}\right\}, \tag{2}$$

where $A=E$, F or G, $k=x$, y or z, and $C=u$, v or w, respectively, and δ_{ij} is the Kronecker delta.

3. Numerical Formulation

The forthcoming subsections briefly describe the finite-volume and temporal discretization of the governing equations.

3.1 Finite-Volume Discretization

The finite volume method (FVM) is used to obtain the solution of the RANS equations. The formulation of the method is obtained by an integration of the flow equations in a finite volume. The application of Gauss theorem for each finite volume yields

$$\int_{V_i}\frac{\partial Q}{\partial t}\,dV+\int_{S_i}\left[\vec{P}_e-\vec{P}_v\right]\cdot d\vec{S}=0\,, \qquad \vec{P}=\vec{P}_e-\vec{P}_v=E\,\vec{i}_x+F\,\vec{i}_y+G\,\vec{i}_z\,, \qquad Q_i=\frac{1}{V_i}\int_{V_i}Q\,dV_i\,. \tag{3}$$

$d\vec{S}$ is the outward oriented normal area vector for the i-th control volume and $\vec{i}_x$, $\vec{i}_y$ and $\vec{i}_z$ are the Cartesian unit vectors, and Q_i is the discrete value of the vector of conserved variables for the i-th control volume V_i.

3.2 Time Integration

Time integration is performed using a Runge-Kutta type scheme similar to the one proposed in Jameson et al. (1981). In the present work, a 2nd-order accurate, 5-stage Runge-Kutta scheme is used, which can be written as

$$\begin{aligned}&Q_i^{(0)}=Q_i^n\,,\\ &Q_i^{(\ell)}=Q_i^{(0)}-\frac{\alpha_\ell\,\Delta t_i}{V_i}\,(CO-VI-DI)_i^{(\ell-1)}\,, \quad \ell=1,...,5\,,\\ &Q_i^{n+1}=Q_i^{(5)}\,.\end{aligned} \tag{4}$$

In the previous equations, CO_i, VI_i and DI_i are, respectively, the convective operator, the viscous operator and the artificial dissipation operator calculated for the i-th control volume. These operators are calculated according to the spatial discretization scheme. The α_ℓ coefficients are $1/4$, $1/6$, $3/8$, $1/2$ and 1 for $\ell=1,\cdots,5$, respectively. The artificial dissipation operator is calculated only on the first, third and fifth stages. For the inviscid calculations, the artificial dissipation operator is calculated in the first and in the second stages.

4. Spatial Discretization

Both centered and upwind schemes are available in the present numerical method for computation of convective fluxes. Viscous fluxes are always computed by a second-order accurate centered scheme in the present paper.

4.1 Centered Scheme

The centered scheme used in this work for spatial discretization was proposed by Jameson et al. (1981). For this scheme, the convective operator is calculated as the sum of the inviscid fluxes on the faces of the i-th volume,which are

computed as a function of the averaged vector of conserved properties at the face, i.e.,

$$CO_i = \sum_{k=1}^{nf} \vec{P}_e\left(Q_k\right) \cdot \vec{S}_k \,, \qquad\qquad Q_k = \frac{1}{2}\left(Q_i + Q_m\right). \tag{5}$$

In this expression, Q_i and Q_m are the conserved properties in the volumes at each side of the k-th face and m indicates the neighbor of the i-th element. The viscous operator in the i-th control volume is calculated as the sum of the viscous fluxes along the faces which constitute the volume.

4.2 First-Order Van Leer Scheme

The convective operator, $C\left(Q_i\right)$, is defined for the van Leer flux vector splitting scheme (van Leer, 1982) by the expression

$$C(Q_i) \;=\; \sum_{k=1}^{nf} \left[E_k \vec{i}_x + F_k \vec{i}_y + G_k \vec{i}_z\right] \cdot \vec{S}_k \,. \tag{6}$$

In the present case, the interface fluxes, E_k, F_k and G_k, are defined as (Azevedo and Figueira da Silva, 1997)

$$E_k \;\; = \;\; \left\{ \begin{array}{ll} E_e^+(Q_i) + E_e^-(Q_m) & \text{for } \vec{S}_k \cdot \vec{i}_x \geq 0 \\ E_e^-(Q_i) + E_e^+(Q_m) & \text{for } \vec{S}_k \cdot \vec{i}_x < 0 \end{array} \right. \tag{7}$$

Here, $E_e^{\pm}(Q_i)$ is the split fluxe calculated using van Leer's formulas (van Leer, 1982) and the conserved properties of the i-th control volume. The F_k and G_k are computed as E_k split fluxe.

The evaluation of the split fluxes in the van Leer context can be summarized as follows:

$$\begin{array}{rcl} M_x \geq 1 & \Rightarrow & E_e^+ \,=\, E_e \;\; \text{and} \;\; E_e^- \,=\, 0 \,, \\ M_x \leq -1 & \Rightarrow & E_e^+ \,=\, 0 \;\; \text{and} \;\; E_e^- \,=\, E_e \,, \\ |M_x| < 1 & \Rightarrow & E_e^{\pm} = \left\{ \begin{array}{c} f^{\pm} \\ f^{\pm}\left[\left(\gamma-1\right)u \pm 2a\right]/\gamma \\ f^{\pm} v \\ f^{\pm} w \\ f^{\pm}\left[\frac{\left\{(\gamma-1)u \pm 2a\right\}^2}{\left\{2(\gamma^2-1)\right\}} + \frac{v^2}{2} + \frac{w^2}{2}\right] \end{array} \right\} . \end{array} \tag{8}$$

$$E_e^{\pm} = \left\{ \begin{array}{c} f^{\pm} \\ f^{\pm}\left[\left(\gamma-1\right)u \pm 2a\right]/\gamma \\ f^{\pm} v \\ f^{\pm} w \\ f^{\pm}\left[\frac{\left\{(\gamma-1)u \pm 2a\right\}^2}{\left\{2(\gamma^2-1)\right\}} + \frac{v^2}{2} + \frac{w^2}{2}\right] \end{array} \right\} .$$

In the previous equations, a is the speed of sound, the Mach number in the x-direction is definedas $M_x = u/a$ and the split mass fluxes are $f^{\pm} = \pm\rho a\left[\left(M_x \pm 1\right)/2\right]^2$. Similar expressions are obtained for $F^{\pm}$ using $M_y = v/a$, and for $G^{\pm}$ using $M_z = w/a$. With this flux vector definition, the splitting is continuosly differentiable at sonic and stagnation points.

4.3 MUSCL Reconstruction

To achive 2nd order accuracy in space for the van Leer and Liou schemes, linear distributions of properties are assumed at each cell to compute te left and right states in the face. Such states are represented by the L and R subscripts, respectively, in the van Leer and Liou definitions. The linear reconstruction of properties is achieved through a MUSCL (Monotone Upstream-Centered Scheme for Conservation Laws) (van Leer, 1979) scheme, in which the property at the interface is obtained through a limited extrapolation using the cell properties and their gradients.

In order to perform such reconstruction at any point inside the control cell, the following expression is used for a generic element, q, of the primitive variable vector, W,

$$q(x,y,z) = q_i + \nabla q_i \cdot \vec{r} \,, \tag{9}$$

where (x,y,z) is a generic point in the $i-$th cell; q_i is the discrete value of the generic property q in the $i-$th cell, which is attributed to the cell centroid, and $\vec{r}$ is the distance vector from the $i-$th cell centroid to a generic point (x,y,z) and ∇q_i is the gradient of the q_i.

4.4 Second-Order Van Leer Scheme

In the present work, the implementation of the 2nd-order van Leer scheme is based on an extension of the Godunov approach. The projection stage of the Godunov scheme, in which the solution is projected in each cell on piecewise constant states, is modified. This constitutes the so-called MUSCL approach (van Leer, 1979) for the extrapolation of primitive variables. By this approach, left and right states at a given interface are linearly reconstructed by primitive variable extrapolation on each side of the interface, together with some appropriate limiting process (Hirsh, 1990) in order to avoid the generation of new extrema, as defined in the previous subsection. The vector of primitive variables is taken as $W = [p, u, v, w, e_i]^T$, in the present case. The convective operator, $C\left(Q_i\right)$, is still defined as in Eq. (6), except that the interface fluxe, $E_k$is now defined as

$$E_k \;=\; \begin{cases} E_e^+(Q_L) + E_e^-(Q_R) & \text{for } \vec{S}_k \cdot \vec{i}_x \geq 0 \\ E_e^-(Q_L) + E_e^+(Q_R) & \text{for } \vec{S}_k \cdot \vec{i}_x < 0 \end{cases} \tag{10}$$

Here, $Q_L = Q(W_L)$ and $Q_R = Q(W_R)$ are the left and right states at the k-th interface obtained by the linear extrapolation process previously discussed. The F_k and G_k are computed as E_k split fluxe.

4.5 First- and Second-Order Liou Schemes

The Liou schemes implemented in this work consider that the flux vectors can be expressed as a sum of the convective and pressure terms(Liou, 1994) and (Liou, 1996). For the construction of the Liou schemes, one can assume that the convective operator may be written as

$$C(Q_i) \;=\; \sum_{k=1}^{nf} \left[E_k n_x + F_k n_y + G_k n_z\right] \cdot \left|\vec{S}_k\right| = \sum_{k=1}^{nf} \left[\left(F_k^{(c)} + P_k\right) |\vec{S}_k|\right] \;, \tag{11}$$

where $F_k^{(c)}$ represents the contribution of the convective terms and P_k represents the pressure terms. Moreover, (n_x, n_y, n_z) are the components of the unit vector normal to the face and oriented outward with regard to the i-th control volume. In order to write the expressions of $F_k^{(c)}$ and P_k, one must initially observe that, for the AUSM$^+$ scheme, the inviscid flux vectors can be written as

$$E_e = u\Phi + P_x \;=\; M_x\, a\, \Phi + P_x \;, \quad F_e = v\Phi + P_y \;=\; M_y\, a\, \Phi + P_y \;, \quad G_e = v\Phi + P_z \;=\; M_z\, a\, \Phi + P_z \;. \tag{12}$$

where the Φ, P_x, P_y and P_z vectors are defined as

$$\Phi = \left\{ \begin{array}{c} \rho \\ \rho u \\ \rho v \\ \rho w \\ \rho H \end{array} \right\} \quad P_x = \left\{ \begin{array}{c} 0 \\ p \\ 0 \\ 0 \\ 0 \end{array} \right\} \quad P_y = \left\{ \begin{array}{c} 0 \\ 0 \\ p \\ 0 \\ 0 \end{array} \right\} \quad P_z = \left\{ \begin{array}{c} 0 \\ 0 \\ 0 \\ p \\ 0 \end{array} \right\} \;. \tag{13}$$

In the previous expressions, p is the pressure, H is the total specific enthalpy, $M_x = u/a$, $M_y = v/a$ and $M_z = w/a$. Hence, one could write that

$$F_k^{(c)} \;=\; \left[\left(un_x + vn_y + wn_z\right)\Phi\right]_k \;, \quad P_k = \left(n_x P_x + n_y P_y + n_z P_z\right)_k \;. \tag{14}$$

The approach followed in the present work in order to extend Liou's ideas(Liou, 1994) to the unstructured grid case consists in defining a local one-dimensional stencil normal to the face considered. For the construction of the first-order scheme, one must identify the "left" (or L) state, as defined in (Liou, 1994) and (Liou, 1996), as the properties of the i-th volume and the "right" (or R) state as those of the m-th volume. The second-order scheme follows exactly the same formulation, except that the left and right states are obtained by a MUSCL extrapolation of primitive variables as described previously in the paper. The *minmod* limiter was again used in this case. The definition of the interface properties follows the standard formulation of the AUSM$^+$ scheme(Liou, 1996). Hence, the interface Mach number, M_k, also according to the definition, can be written as

$$M_k = M_L^+ + M_R^- \;, \tag{15}$$

where $M_L^+ = M^+(M_L)$ and $M_R^- = M^-(M_R)$. The split Mach numbers are defined as

$$M_L^+ = \left\{ \begin{array}{ll} \frac{1}{2}\left(M_L + |M_L|\right) & \text{, if } |M_L| \geq 1, \\ M_\beta^+(M_L) & \text{, otherwise,} \end{array} \right. \;, \quad M_R^- = \left\{ \begin{array}{ll} \frac{1}{2}\left(M_R - |M_R|\right) & \text{, if } |M_R| \geq 1, \\ M_\beta^-(M_R) & \text{, otherwise.} \end{array} \right. \tag{16}$$

The $M_\beta^\pm$ terms can be written as

$$M_\beta^\pm(M) \;=\; \pm\frac{1}{4}(M \pm 1)^2 \;\pm\; \beta(M^2 - 1)^2 \;. \tag{17}$$

This work used $\beta = 1/8$, as suggested in Liou (1994). Moreover, in order to achieve a unique splitting in Liou's sense, the left and right Mach numbers are defined as

$$M_L = \frac{\tilde{V}_L}{a_k} \quad \text{and} \quad M_R = \frac{\tilde{V}_R}{a_k} \,, \tag{18}$$

where

$$\begin{aligned} \tilde{V}_L &= u_L n_x + v_L n_y + w_L n_z \,, \\ \tilde{V}_R &= u_R n_x + v_R n_y + w_R n_z \,. \end{aligned} \tag{19}$$

The corresponding speed of sound, a_k, at the interface is given by

$$a_k = \min\left(\tilde{a}_L \,,\, \tilde{a}_R\right) \,, \qquad \tilde{a}_L = a_L^* \cdot \min\left(1 \,,\, \frac{a_L^*}{\left|\tilde{V}_L\right|}\right) \,, \qquad a_L^* = \sqrt{\frac{2(\gamma-1)}{(\gamma+1)}\, H_L} \,, \tag{20}$$

and a similar definition for $\tilde{a}_R$. The pressure, p_k, at the k-th interface is given by

$$p_k \,=\, p_L^+ \, p_L \,+\, p_R^- \, p_R \,. \tag{21}$$

The split pressures, still following the expressions in Liou (1994), can be written as

$$p_L^+ = \begin{cases} \frac{1}{2}\left(1 \,+\, \text{sign}(M_L)\right) & \text{, if } |M_L| \geq 1, \\ p_\alpha^+(M_L) & \text{, otherwise,} \end{cases} \quad , \quad p_R^- = \begin{cases} \frac{1}{2}\left(1 \,-\, \text{sign}(M_R)\right) & \text{, if } |M_R| \geq 1, \\ p_\alpha^-(M_R) & \text{, otherwise.} \end{cases} \tag{22}$$

The $p_\alpha^\pm$ terms can be written as

$$p_\alpha^\pm(M) \,=\, \frac{1}{4}(M \pm 1)^2(2 \mp M) \,\pm\, \alpha M (M^2-1)^2 \,. \tag{23}$$

This work used $\alpha = 3/16$, as suggested in Liou (1994). Therefore, with the interface properties so defined and using Eq. (14), the $F_k^{(c)}$ and P_k vectors can be finally written as

$$F_k^{(c)} \,=\, \frac{1}{2}\, M_k \, a_k \left(\Phi_L + \Phi_R\right) \,-\, \frac{1}{2}\, |M_k| \, a_k \left(\Phi_R - \Phi_L\right) \,, \tag{24}$$

and

$$P_k = \left\{ \begin{array}{c} 0 \\ p n_x \\ p n_y \\ p n_z \\ 0 \end{array} \right\} \,. \tag{25}$$

Hence, the convective operator, $C(Q_i)$, can be computed using Eq. (11).

5. Results and Discussion

A 3-D inlet configuration which is representative of some proposed inlet geometries for a typical transatmospheric vehicle was used as a test in the present work, as we can observe in Fig.1(a).

For the present simulations, the fluid was treated as a perfect gas with constant specific heat and no chemistry was taken into account. The purpose of these simulations is to compare the different schemes applied to high Mach number flows in order to verify if they are able to represent all flow features, such as strong shocks, shock reflections and interactions, and expansion regions. Moreover, there is interest in verifying whether the schemes can avoid oscillations in the presence of such strong discontinuities.

A computional mesh comparative study is very important and is part of the presente work. The influence of the results is observed for three grids made up of prism elements. In Fig. 1(b), one can observe the 2-D view of the meshes used in this study. The pressure coefficient for the 2nd-order upwind van Leer scheme is compared with the available analytical solutions, which are valid upstream of the shock interactions, using diferent grids to observe the influence of the mesh in the pressure coefficient distribution in the upper and lower surface of the configuration. The first grid is made up of 5716 prism volumes, the second grid has 24045 volumes and the third grid has 60937 volumes. One can observe that only the second and the third grids given an acceptable pressure coefficient distribution results. For this instance, all the results performed in this paper are computed using the more fine grid with 60937 volumes.

The pressure coefficient distribution results with the 2nd-order centered scheme, the 1st- and 2nd-order van Leer schemes, and the 1st- and 2nd-order Liou schemes are shown in Figs. 3(a) and 3(b). One can observe that the upper wall

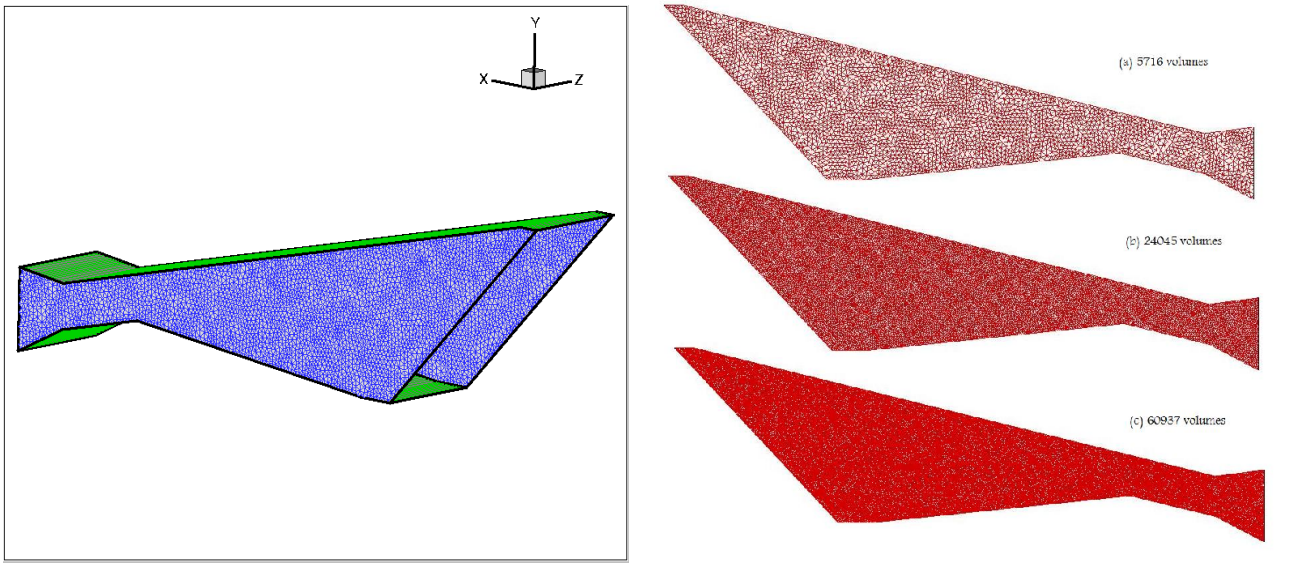

(a) 3-D inlet configuration. (b) 2-D view of the grids.

Figure 1. 3-D Unstructured grids made up of prism elements.

schock and the lower wall schock are less oscillatory in the computations with the 1st-order van Leer upwind scheme. This is to be expected since this scheme is quite a bit more diffusive than the other schemes tested in the paper.

The shock positions have been fairly well captured for all test cases presented in this paper. It is also correct to state that the results for the upper wall shocks seem to be slightly better resolved than those for the lower wall. In general, good qualitative results are obtained with the present numerical tool. The more diffusive character of 1st-order schemes is evident in the quantitative results presented. Pressure coefficient distributions calculated indicate that the additional numerical diffusivity of 1st-order schemes can destroy some of the information in the downstream regions. Moreover, it is also clear that the upper wall entrance shock is more sharply defined by the 2nd-order upwind solutions than by the 2nd-order centered scheme and the 1st-order upwind calculations.

In Figs. 4(a) and 4(b), one can observe the pressure and Mach number contours respectively for $M_\infty = 4$ using the 2nd-order van Leer upwind scheme. In the contours we can observe the shock-shock interactions in the downstream portion of the flow and that the overall flow features are well captured by the scheme. Similar results were found with simulations considering inlet entrance Mach numbers $M_\infty = 8$ and $M_\infty = 12$ and the results are not included in this paper.

6. Concluding Remarks

The present work intends the perform a comparison of five different spatial discretizations schemes for cold gas hypersonic flow simulations. The schemes here presented are applied to the solution of supersonic and hypersonic inlet flows. The results included in the present paper only considered inviscid computations,and the fluid was treated as a perfect gas. In actual flight, an inlet flow with a high entrance Mach number could not be simulated with the perfect gas assumption. In other words, real gas behavior would have to be taken into account. From a physical standpoint, however, the present calculations could be considered as the simulation of the cold gas flows which are usually achieved in experimental facilities such as gun tunnels. simulations could be seen as a necessary step in the construction of a robust code to deal with the complete environment encountered in actual flight. Here, however, the consideration of very high Mach number flows has simply the objective of testing the behavior of the different schemes in the presence of strong shocks.

The equations are advanced in time by an explicit, 5-stage, 2nd-order accurate, Runge-Kutta time stepping procedure. The spatial discretization considers a centered scheme and two upwind schemes, namely van Leer and Liou flux-vector splitting schemes, with both 1st- and 2nd-order implementations. The implementation of the 2nd-order versions of the two upwind schemes uses MUSCL reconstruction in order to obtain left and right states at interfaces. The 1st-order van Leer flux vector splitting scheme has reduced the flow property oscillations. However, as one could expect, this 1st-order method also causes considerable smearing of the flow discontinuities due to the excessive artificial dissipation intrinsically added.

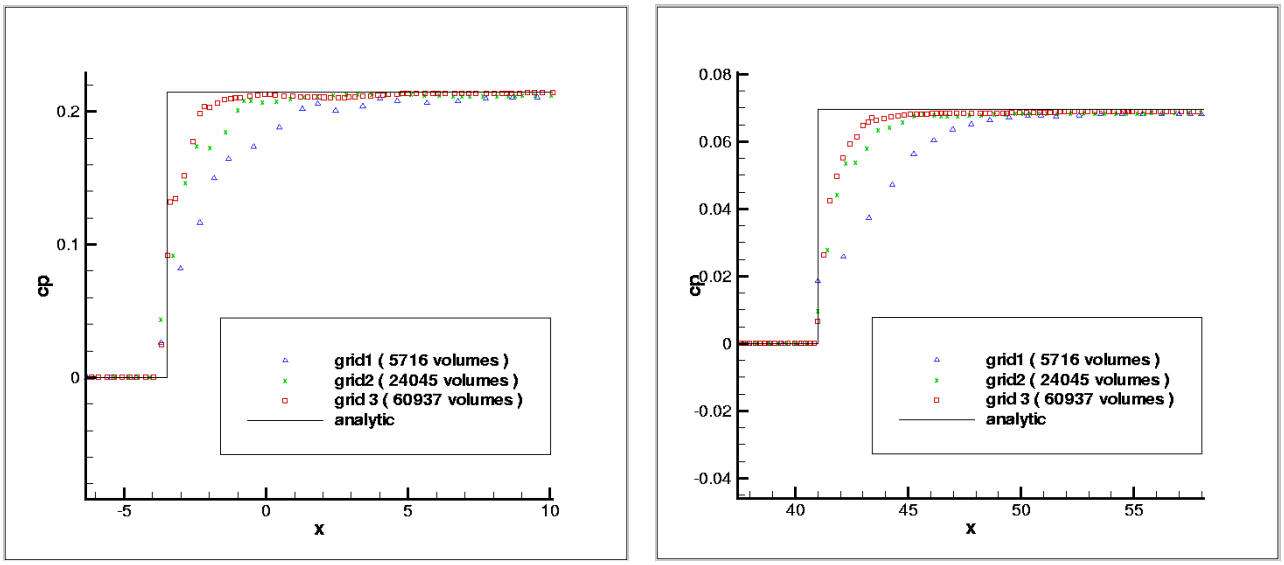

(a) Upper wall. (b) Lower wall.

Figure 2. Study of grid influence in the pressure coefficient distributions in the lower and upper walls for $M_\infty = 4$.

7. Acknowledgments

The authors gratefully acknowledge the support of Fundação de Amparo à Pesquisa do Estado de São Paulo, FAPESP, through a M.S. Scholarship for the first author under the FAPESP Grant No. 03/10209-2.

8. REFERENCES

Anderson, W. K. and Thomas, J. L. and van Leer, B.,"A Comparison of Finite Volume Flux Vector Splittings for the Euler Equations," *AIAA Journal*, Vol. 24, No. 9, Sept. 1986, pp. 1453-460.

Azevedo, J. L. F. and Figueira da Silva, L. F.,"The Development of an Unstructured Grid Solver for Reactive Compressible Flow Applications," AIAA Paper 97-3239, *33rd AIAA/ASME/SAE/ASEE Joint Propulsion Conference & Exhibit*, Seattle, WA, July 1997.

Hirsch, C.,"Numerical Computation of Internal and External Flows," *Computational Methods for Inviscid and Viscous Flows*, Vol. 2, Wiley, New York, 1st ed., 1990, pp. 408-443.

Jameson, A. and Schmidt, W. and Turkel, E.,"Numerical Solution of the Euler Equations by Finite Volume Methods Using Runge-Kutta Time-Stepping Schemes," AIAA Paper 81-1259, *14th AIAA Fluid and Plasma Dynamics Conference*, Palo Alto, CA, June 1981.

Liou, M.-S.,"A Continuing Search for a Near-Perfect Numerical Flux Scheme. Part I: AUSM$^+$'" NASA TM-106524, Mar. 1994.

Liou, M.-S.,"A Sequel to AUSM: AUSM$^+$,"*Journal of Computational Physics*, Vol. 129, No. 2, 1996, pp. 364-382.

Pulliam, T. H. and Steger, J. L.,"Implicit Finite-Difference Simulations of Three-Dimensional Compressible Flow,"*AIAA Journal*, Vol. 18, No. 2, Feb. 1980, pp. 159-167.

Steger, J. L. and Warming, R. F., "Flux Vector Splitting of the Inviscid Gasdynamic Equations with Application to Finite-Difference Methods," *Journal of Computational Physics*, Vol. 40, No. 2, Apr. 1981, pp. 263-293.

van Leer, B.,"Towards the Ultimate Conservative Difference Scheme. V. A Second-Order Sequel to Godunov's Method,"*Journal of Computational Physics*, Vol. 32, No. 1, July 1979, pp. 101-136.

van Leer, B.,"Flux-Vector Splitting for the Euler Equations,"*Proceding of the 8th International Conference on Numerical Methods in Fluid Dynamics, Lecture Notes in Physics*, Vol. 170, Springer-Verlag, Berlin, 1982, pp. 507–512.

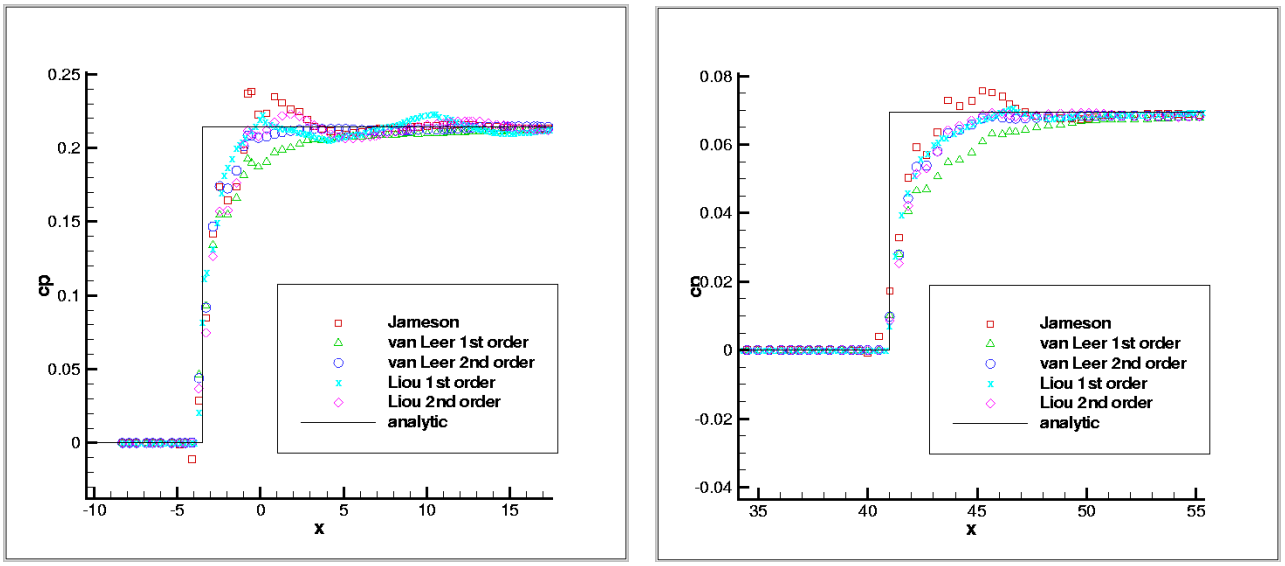

(a) Upper wall. (b) Lower wall.

Figure 3. Pressure coefficient distributions in the lower and upper walls for $M_\infty = 4$.

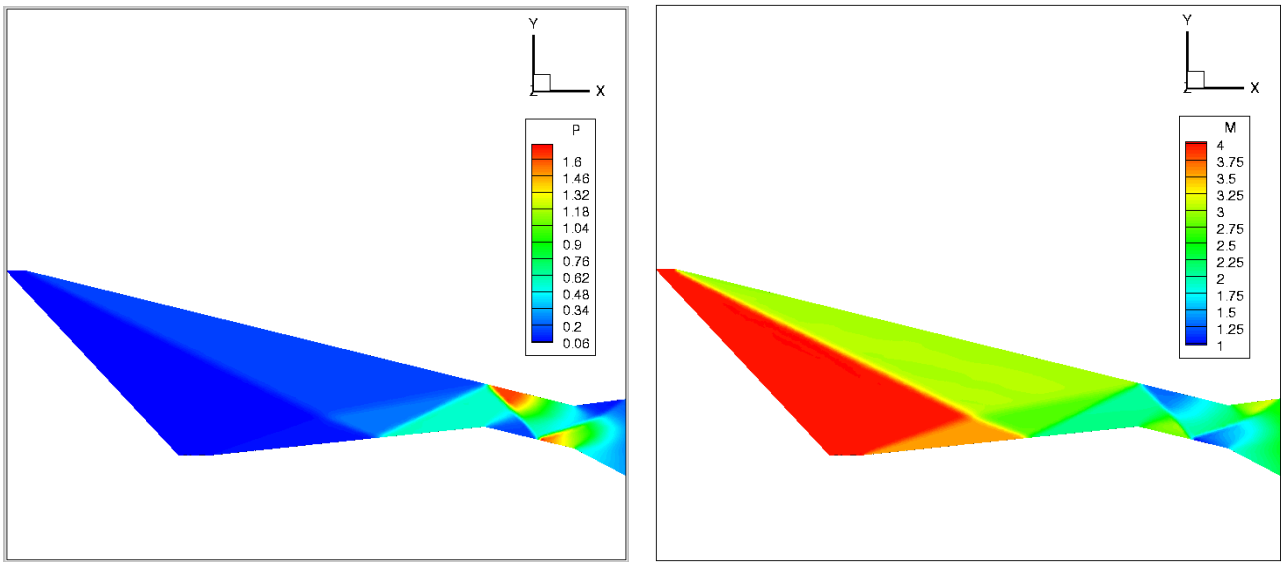

(a) Pressure. (b) Mach number.

Figure 4. Pressure and Mach number contours obtained for the 2nd-order van Leer scheme ($M_\infty = 4$).